

# Insights into the Chloramphenicol Inhibition Effect on Peptidyl Transferase Activity, Using Two New Analogs of the Drug

Ourania N. Kostopoulou<sup>1</sup>, Theodoros G. Kourelis<sup>1</sup>, Petros Mamos<sup>1</sup>, George E. Magoulas<sup>2</sup> and Dimitrios L. Kalpaxis<sup>1,\*</sup>

<sup>1</sup>Laboratory of Biochemistry, School of Medicine, University of Patras, 26504- Patras, Greece; <sup>2</sup>Laboratory of Synthetic Organic Chemistry, Department of Chemistry, School of Natural Sciences, University of Patras, 26504- Patras, Greece

**Abstract:** Chloramphenicol (CAM) inhibits peptide bond formation by binding to the 50S subunit of prokaryotic ribosomes and interfering competitively with the binding of the aminoacyl-tRNA 3'- terminus to ribosomal A-site. Further studies have demonstrated that CAM (I) reacts rapidly with a model initiator ribosomal complex [poly(U)-programmed ribosomes from *Escherichia coli*, bearing AcPhe-tRNA at the P-site], complex C, to form an encounter complex CI which is then isomerized slowly to a tighter complex, C<sup>\*</sup>I. Herein, we show by time-resolved footprinting analysis that CAM produces a footprint in CI complex, comprising nucleotides A2451, G2505, and U2506, all exhibiting reduced reactivity against base-specific modifying agents. When C<sup>\*</sup>I complex is footprinted, the reactivities of G2505 and U2506 are almost restored, while protection is observed at A2062 and altered reactivity at A2058 and A2059. Our results suggest that CAM initially binds to a hydrophobic crevice composed of nucleotides located adjacently to the A-site (CI complex). Soon after, CAM shifts slowly to a final position, in which the interaction between the p-nitrobenzyl group of CAM and the base of A2451 is conserved, while the dichloroacetyl group reorientates toward A2062. Analogous behavior is observed, if CAM is modified by replacement of dichloroacetyl group with  $\beta$ -alanyl. However, insertion at this position of a bulkier group, such as phenylalanyl-phenylalanyl group, sterically prevents CAM accommodation to its initial binding site and favors its direct fitting into the final binding pocket. Our data correlate well with recent crystallographic results regarding CAM binding on *Thermus thermophilus* and *E. coli* ribosomes.

**Keywords:** Chloramphenicol, chloramphenicol derivatives, slow binding inhibitors, puromycin reaction, ribosome, 23S rRNA, peptidyl transferase, ribosomal A-site, peptide exit-tunnel.

## INTRODUCTION

Chloramphenicol (CAM) is a broad spectrum antibiotic with high potency in fighting certain anaerobic bacteria and bacteria infecting the central nervous system. Despite its potential toxicity to the hematopoietic system [1], CAM has been the preferred drug for the topical treatment and prevention of superficial eye infections [2]. CAM exerts its bactericidal effect by binding to the peptidyl transferase (PTase) region of the 50S ribosomal subunit and blocking essential ribosomal functions, such as PTase activity [3-6], binding and movement of tRNAs through the ribosome [7, 8], and peptide termination [9, 10]. CAM has been considered as interfering competitively with the binding of the 3'-end of aminoacyl-tRNA to ribosomal A-site. In favor of this view is the observation that CAM competes with puromycin, an antibiotic regarded as iso-structural with the 3'- terminus of aminoacyl-tRNA, for binding to 70S ribosomes [11], and inhibits competitively the peptide bond formation between puromycin and P-site bound acetylphenylalanyl-tRNA (AcPhe-tRNA) [3, 6]. Crystallographic studies have also indicated that CAM complexed to either 50S ribosomal

subunits of *Deinococcus radiodurans* or 70S ribosomes of *Thermus thermophilus* and *E. coli*, binds to the A-site crevice [12-14]. Nevertheless, single-site mutations of 11 different nucleotides in the V-loop of 23S rRNA can confer CAM resistance [15, 16], while at least 5 nucleotides within this region exhibit altered reactivity against chemical modification when CAM is bound [17, 18]. These positions show minimal overlap with those related with puromycin binding. Moreover, Hansen *et al.*, have indicated through X-ray crystallography in *Haloarcula marismortui* 50S subunits that CAM binds to a hydrophobic crevice at the entrance to the peptide exit tunnel [19], while Long and Porse using a crosslinking approach suggested that a similar binding site is present on the *E. coli* ribosome [20]. These observations reinforce early equilibrium dialysis measurements providing evidence that CAM binds to two sites on the 50S subunit; one of high affinity ( $K_D = 2 \mu\text{M}$ ) and another of low affinity ( $K_D = 200 \mu\text{M}$ ) [21].

In this study, we re-examine the complicated behavior of CAM, following two approaches. First, since CAM interacts with a model initiator ribosomal complex [poly(U)-programmed ribosomes bearing AcPhe-tRNA at the P-site], complex C, *via* a two-step mechanism, we apply a time-resolved chemical probing to achieve a complete picture of the entire course of CAM binding to *E. coli* ribosomes. Second, aiming at correlating the electronegativity and/or

\*Address correspondence to this author at the Laboratory of Biochemistry, School of Medicine, University of Patras, 26504-Patras, Greece;  
Tel: + 302610-996124; Fax: + 302610-969167;  
E-mail: dimkal@med.upatras.gr

polarizing action of the aminoacyl group with the inhibitory potency of CAM on peptide bond formation, we analyze the inhibition of the puromycin reaction by two derivatives of CAM,  $\beta$ -alanyl-CAM ( $\beta$ -Ala-CAM) and phenylalanyl-phenylalanyl-CAM (Phe-Phe-CAM), that have the dichloroacetyl group replaced by  $\beta$ -alanine and phenylalanyl-phenylalanine, respectively (Fig. (1)). Using these approaches, we show that CAM initially binds to a low affinity site and protects nucleotides A2451, G2505 and U2506 from chemical modification. Soon after this initial binding, CAM shifts to a high-affinity site, without losing its interaction with A2451. From this position, CAM affects the sensitivity of nucleotides A2062, A2058 and A2059 against dimethyl-sulfate (DMS). Furthermore, we show that substitution of the dichloroacetyl moiety of CAM by amino acid or dipeptide group can change the potency and the mode of binding of the drug.

## MATERIALS AND METHODS

### Materials

Puromycin dihydrochloride, CAM, CAM free base [D-(-)-*threo*-1-(*p*-nitrophenyl)-2-amino-1,3-propanediol], tRNA<sup>Phe</sup> from *E. coli*, DMS and DMS stop solution were purchased from Sigma-Aldrich, while ketoxal and 1-cyclohexyl-3-(2-morpholinoethyl)-carbodiimide metho-*p*-toluene sulfate (CMCT) from MP Biomedicals and Fluka Biochemicals, respectively. AMV reverse transcriptase, dNTPs and ddNTPs were supplied by Roche Diagnostics, while L-[2,3,4,5,6 - <sup>3</sup>H]Phenylalanine and [ $\alpha$ -<sup>32</sup>P]ATP were from Amersham Biosciences.

### Synthesis of CAM Derivatives

Synthesis of D-(-)-*threo*-1-(*p*-nitrophenyl)-2-( $\beta$ -alanyl-amido)-1,3-propanediol ( $\beta$ -Ala-CAM). CAM free base (6.7 g, 31.53 mmol) was dissolved in dry dimethylformamide (DMF) (30 mL). Hydroxysuccinimide ester of trityl- $\beta$ -alanine (12.85 g, 30 mmol) prepared as described previously [22] and diisopropyl-ethylamine (DIPEA) (5.39 mL, 30.9 mmol) were added to the above solution in two portions stirring. The mixture was stirred at RT for 24 h, and then at 60 °C for

1 h. The resulting solution was partitioned between 200 mL of dichloromethane and 70 mL H<sub>2</sub>O. The organic layer was washed twice with 50 mL of an aq. solution 5% citric acid, and twice with 50 mL of a saturated solution of NaCl. The organic layer was dried over MgSO<sub>4</sub> and evaporated *in vacuo*. The resulting powder was recrystallized from ethyl acetate and yielded 22 mmol of trityl- $\beta$ -alanyl-CAM crystals. An aliquot of the above product (10 mmol) was dissolved in 15 mL of a solution of 2.85 g (15 mmol) of toluene-4-sulfonic acid monohydrate in isopropyl alcohol. The mixture was heated at 60 °C for 20 min, and the tosylate was crystallized by keeping at RT overnight. The crystals were filtered under vacuum, washed with small aliquots of ether, and recrystallized from isopropyl alcohol. The yield was 7 mmol (70%) of the  $\beta$ -alanyl-CAM tosylate. Free base of  $\beta$ -alanyl-CAM was obtained from its tosylate as described by Drinas *et al.*, [23]. Then, 0.85 g (3 mmol) of free base was partitioned between 50 mL of ethyl acetate, and 8 mL of an aq. solution 10% sodium carbonate. The organic phase was washed three times with 10 mL of a saturated solution of NaCl, dried over MgSO<sub>4</sub>, and evaporated *in vacuo*. The yield was 0.34 g (40%) of  $\beta$ -alanyl-CAM. <sup>1</sup>H NMR (MeOH-*d*<sub>4</sub>): 8.26 (2H, d, *J* = 8.8 Hz), 7.71 (2H, d, *J* = 8.8 Hz), 5.17 (1H, d, *J* = 2.4 Hz), 3.82-3.77 (1H, m), 3.66 (1H, dd, *J* = 7.2 and 11.2 Hz), 3.37 (1H, dd, *J* = 7.2 and 11.2 Hz), 3.23-3.19 (2H, m), 3.12-3.07 (2H, m) ppm.

Synthesis of D-(-)-*threo*-1-(*p*-nitrophenyl)-2-(phenylalanyl-L-phenylalanyl-amido)-1,3-propanediol (Phe-Phe-CAM). The dipeptidyl derivative of CAM, Phe-Phe-CAM, was synthesized as reported previously [23]. <sup>1</sup>H NMR (MeOH-*d*<sub>4</sub>): 8.25 (2H, d, *J* = 8.8 Hz), 7.59 (2H, d, *J* = 8.8 Hz), 7.31-7.12 (10H, m), 5.13 (1H, d, *J* = 2.4 Hz), 4.88-4.83 (1H, buried under solvent), 4.15-4.12 (1H, m), 3.99 (1H, t, *J* = 4.8 Hz), 3.86-3.81 (1H, m), 3.69-3.65 (2H, m), 3.54-3.50 (1H, m), 3.12-3.09 (1H, m), 2.88-2.85 (1H, m) ppm.

### Biochemical Preparations

70S ribosomes were prepared from *E. coli* K12 cells as described previously [24]. Ac[<sup>3</sup>H]Phe-tRNA charged to 85% and complex C bearing Ac[<sup>3</sup>H]Phe-tRNA at the P-site were

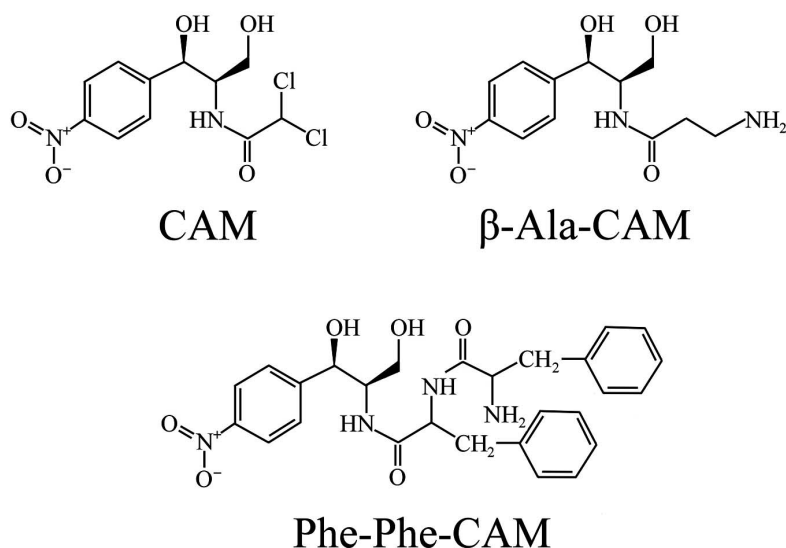


Fig. (1). Chemical structures of CAM,  $\beta$ -Ala-CAM and Phe-Phe-CAM.

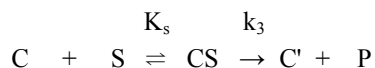
prepared and purified as shown in the previous reference. The percentage of ribosomes, active in AcPhe-tRNA binding, was 72%. This ribosomal population was more than 90% reactive towards puromycin.

### Time Resolved Binding of CAM to Complex C

Complex C at 100 nM was incubated alone or with 50  $\mu$ M CAM ( $50 \times K_i$ ) in 100  $\mu$ l of buffer A [Hepes/KOH, pH 7.2, 10 mM Mg(CH<sub>3</sub>COO)<sub>2</sub>, 100 mM NH<sub>4</sub>Cl, and 5 mM dithiothreitol] at 25 °C, either for 2 s (CI probing) or for 2 min (C\*I probing). Complexes CI and C\*I were then probed at 37 °C for 10 min with DMS, kethoxal, or CMCT, as described elsewhere [25]. Reactions were stopped and the ribosomal RNA (rRNA) was recovered from ribosomal complexes by extracting twice with phenol, once with chloroform and precipitating with ethanol, before redissolving in Milli-Q water. The sites of modifications in 23S rRNA were analyzed by primer extension with reverse transcriptase, according to Stern *et al.*, [26]. The primers were complementary to the sequences 2099-2116 and 2561-2576 of 23S rRNA. Extension products were run on 6% polyacrylamide/7M urea gels. The positions of modified nucleotides were identified with reference to sequencing reactions performed on an unmodified rRNA template. Band intensities were quantified by phosphorimaging (Fujifilm, FLA-3000, Berthold; Image Quant Software AIDA, Raytest) and averaged over three replications. The variability between lanes was corrected using the relative intensity of a band corresponding to a nucleotide whose accessibility to the chemical probe was not affected by the drug binding. Each value indicated in Table 1 denotes the ratio between the intensity of a band of interest and the intensity of the corresponding band obtained in the absence of CAM.

### Inhibition of Peptide Bond Formation by CAM Derivatives

The reaction between complex C and excess puromycin (S), a pseudo-substrate which binds to the ribosomal A-site, was performed at 25 °C in buffer A [100 mM Tris/HCl, pH 7.2, 10 mM Mg(CH<sub>3</sub>COONa)<sub>2</sub>, 100 mM NH<sub>4</sub>Cl, 6 mM  $\beta$ -mercaptoethanol]. Under these conditions, the puromycin reaction,



displays pseudo-first-order kinetics [5]. The product, Ac[<sup>3</sup>H]Phe-puromycin (P), was extracted by ethyl acetate and its radioactivity was measured in a liquid scintillation spectrometer. The product expressed as the percentage (x) of complex C radioactivity added in the reaction mixture, was appropriately corrected [6] and fitted into equation 1,

$$\ln[100/(100 - x)] = k_{obs} \cdot t \quad (1)$$

The pseudo-first-order rate constant,  $k_{obs}$ , was related to the puromycin concentration, [S], by the relationship

$$k_{obs} = k_3 [S] / (K_s + [S]) \quad (2)$$

The values of  $k_3$  and  $K_s$  were estimated from the double-reciprocal plot of equation 2 by linear regression.

In the presence of either  $\beta$ -Ala-CAM or Phe-Phe-CAM, biphasic logarithmic time plots were obtained. The slope of the straight line through the origin, called initial slope, was taken as the value of the apparent rate constant,  $(k_{obs})_o$ , at the early phase of the reaction, while the slope of the second straight line was taken as the value of the rate constant,  $(k_{obs})_s$ , at the late phase of the reaction.

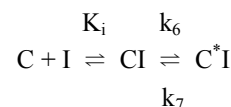
### Statistics

All data indicated in the figures denote the mean values obtained from 3 experiments. One-way ANOVA was used to estimate the mean values and data variability. Statistical tests were performed using the program SPSS Statistics 17.0.

## RESULTS

### Stepwise Binding of CAM to Complex C

As indicated previously [6], CAM binds to complex C in a two-step process, following the kinetic scheme:



According to that study, the formation of the encounter complex CI at 6 mM Mg<sup>2+</sup> is established rapidly, while the isomerization step is accomplished slowly [6]. In agreement with those results, the binding of CAM to complex C at 10 mM Mg<sup>2+</sup> proceeds *via* the same mechanism. Comparing the  $K_i$  values, we conclude that at 10 mM Mg<sup>2+</sup> the affinity of CAM for complex C during the initial step of binding becomes higher than that previously measured at 6 mM Mg<sup>2+</sup>

**Table 1. Equilibrium and Kinetic Constants of the Inhibition of Puromycin Reaction by CAM and its Derivatives**

Constant	CAM	$\beta$ -Ala-CAM	Phe-Phe-CAM
$K_i$ ( $\mu$ M)	0.80 $\pm$ 0.11	45.80 $\pm$ 6.60	
$K_i^*$ ( $\mu$ M)	0.24 $\pm$ 0.03	10.06 $\pm$ 2.22	45.46 $\pm$ 5.55
$k_6/k_7$	2.33 $\pm$ 0.43	3.55 $\pm$ 0.93	
$k_6$ ( $\text{min}^{-1}$ )	2.30 $\pm$ 0.08	2.84 $\pm$ 0.83	
$k_7$ ( $\text{min}^{-1}$ )	0.98 $\pm$ 0.05	0.80 $\pm$ 0.02	
$k_{on}$ ( $\mu\text{M}^{-1} \text{min}^{-1}$ )			(1.87 $\pm$ 0.21) $\times 10^{-2}$
$k_{off}$ ( $\text{min}^{-1}$ )			0.84 $\pm$ 0.03

(Table 1). Nevertheless, the concentration of  $Mg^{2+}$  does not influence the  $k_6$  and  $k_7$  constants of the subsequent isomerization step. The apparent association rate constant of CAM binding,  $(k_6 + k_7)/K_i$ , at 10 mM  $Mg^{2+}$  and 100 mM  $NH_4^+$  equals  $6.8 \times 10^4 M^{-1} s^{-1}$ , a value much lower than the upper limit of  $10^6 M^{-1} s^{-1}$ , set for the characterization of a drug as a slow-binding inhibitor [27].

Based on these observations, we followed a kinetic footprinting approach, successfully applied in studying the interactions of other slow-binding inhibitors with *E. coli* ribosomes [25, 28]. To footprint the CI complex, CAM and complex C were incubated at 25 °C for 2 s, and then probed with chemical reagents for 10 min to modify nucleotides of interest in 23S rRNA. It is noteworthy that the chemical

probes used react with accessible nucleotides within a few milliseconds [29]. Since the equilibrium  $C + I \rightleftharpoons CI$  is established instantaneously while the second step proceeds slowly, the main product provided during the time interval of 2 s is complex CI ( $\approx 90\%$ ). To footprint the C\*I complex, the incubation time of complex C with CAM was extended over nine half lives ( $t_{1/2}$ ). Because the isomerization constant is 2.3, most of the added complex C at the end of this time interval should be in the form of complex C\*I. Representative autoradiograms obtained by primer extension analysis, are shown in Fig. (2). Relative reactivities of the modified nucleotides by the probes are summarized in Table 2. CAM at the CI binding stage strongly protects A2451, G2505 and U2506. After longer exposure of complex C to CAM, the

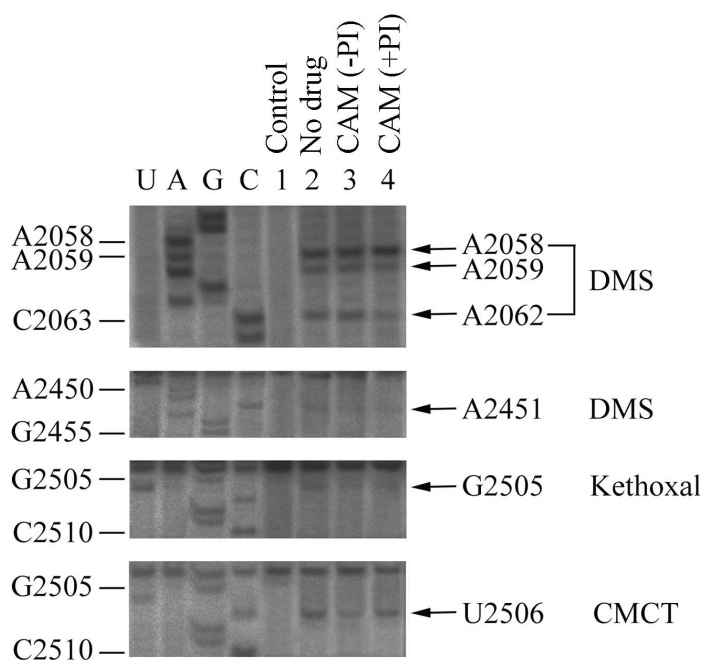


**Fig. (2).** Protections against chemical probes in nucleotides of the central loop of domain V of 23S rRNA, caused by CAM binding to complex C. Antibiotic binding was performed for 2 s (-PI) or 2 min (+PI) in buffer A. The resulting complexes were then probed with DMS, kethoxal, or CMCT. The modification sites were detected by primer extension analysis. U, A, G and C are dideoxy sequencing lanes. Lane 1, unmodified complex C; lane 2, modified complex C, in the absence of CAM; lane 3, complex C reacting with CAM for 2 s (-PI) and then modified; lane 4, complex C reacting with CAM for 2 min (+PI) and then modified. Numbering of nucleotides for the sequencing lanes is indicated at the left. Nucleotides with accessibility affected by bound antibiotic are indicated by arrows at the right. AMV reverse transcriptase stops one position before a modified nucleotide [26].

**Table 2. Footprinting of the CAM Binding Sites in the Central Loop of Domain V of 23S rRNA, at the Initial (CI) and the Final (C\*I) Binding State**

23S rRNA Residue	C	CI	C*I
A2058	1	1.00 ± 0.05	1.35 ± 0.10
A2059	1	1.00 ± 0.08	0.70 ± 0.08
A2062	1	1.00 ± 0.07	0.40 ± 0.11
A2451	1	0.50 ± 0.15	0.52 ± 0.13
G2505	1	0.62 ± 0.11	0.70 ± 0.07
U2506	1	0.75 ± 0.11	0.88 ± 0.07

Relative reactivity of nucleotides denotes the ratio between the intensity of a band of interest and the intensity of the corresponding band obtained in the control lane (complex C in the absence of CAM). Only positions, in which binding of CAM changes the base reactivity, are shown. Data represent the mean ± S.E values obtained from three independently performed experiments.

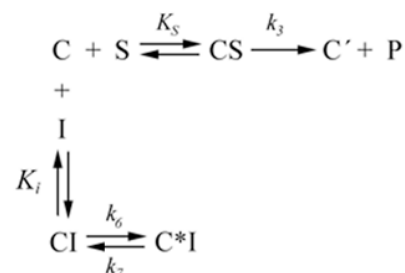
protection effects appear on A2062 and A2059, while the accessibility of A2058 is enhanced.

### Inhibition of the Puromycin Reaction by CAM Derivatives

Because the reaction between complex C and puromycin in excess proceeds under single turnover conditions, it displays pseudo-first-order kinetics. In accordance, equation 1 predicts that the progress curve of the puromycin reaction ( $\ln [100/(100-x)]$  versus  $t$ ) is a straight line. A representative plot obtained at 400  $\mu\text{M}$  puromycin is shown in Fig. (3A) (upper line). However, when the puromycin reaction is performed in the presence of  $\beta$ -Ala-CAM, two phases can be clearly seen in the progress curves, the first one proceeding much faster than the subsequent one Fig. (3A), four lower lines. Moreover, the initial slope of progress curves varies as a function of  $\beta$ -Ala-CAM concentration. This inhibition pattern is reminiscent of that previously obtained with CAM in buffer containing 6 mM  $\text{Mg}^{2+}$  [6] and suggests that  $\beta$ -Ala-CAM, like the parent compound, binds rapidly to complex C to form the encounter complex CI, which then undergoes a slow conformational change to form a tighter complex, termed C\*I. A kinetic model explaining the above-mentioned results can be described by Scheme 1.

Further supporting evidence for the consistency of this model with our kinetic results is provided by the observation that inhibition at both phases (early and late), is of the simple competitive type (Fig. (3B, C)), and second from plots of the

apparent equilibration rate constant (see Appendix),  $k'$ , versus  $\beta$ -Ala-CAM concentration. As shown in Fig. (3D), such a plot is hyperbolic, in agreement with a two-step inhibition mechanism. According to the slow-onset inhibition theory [27], the values of  $k'$  can be estimated from the intersection point of the two linear extrapolations of each progress curve; at this point,  $k' = 1/t$ . The values of  $k_6$  and  $k_7$  can be estimated from the plots as shown in Fig. (3D), by non-linear regression. Mean values of  $k_6$  and  $k_7$  constants, as well as mean values of  $K_i$  and  $K_i^*$ , concerning the early and late phases of inhibition, are given in Table 1.



**Scheme 1.** Kinetic model for the inhibition of the puromycin reaction by  $\beta$ -Ala-CAM. Symbols: C, poly(U)-programmed ribosomes from *E. coli*, bearing AcPhe-tRNA at the P-site; S, puromycin; P, AcPhe-puromycin; C', a form of complex C not recycling; I,  $\beta$ -Ala-CAM

When Phe-Phe-CAM is used as an inhibitor of the puromycin reaction, biphasic logarithmic time plots are also

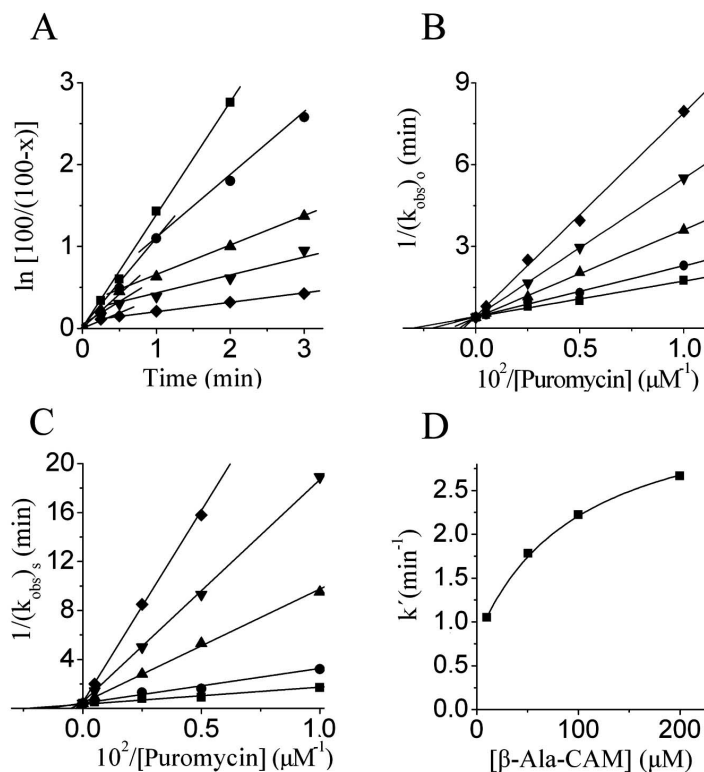


**Fig. (3).** Kinetics for the AcPhe-puromycin synthesis in the presence or absence of  $\beta$ -Ala-CAM. **A**, First-order time plots; Complex C reacted at 25  $^{\circ}\text{C}$  with ( $\blacksquare$ ) 400  $\mu\text{M}$  puromycin or with a solution containing 400  $\mu\text{M}$  puromycin and  $\beta$ -Ala-CAM at ( $\bullet$ ) 10  $\mu\text{M}$ , ( $\blacktriangle$ ) 50  $\mu\text{M}$ , ( $\blacktriangledown$ ) 100  $\mu\text{M}$  and ( $\blacklozenge$ ) 200  $\mu\text{M}$ . **B** and **C**, Double-reciprocal plots; The data were collected from the early and the late phases of logarithmic time plots, respectively, such as those shown in panel A. **D**, Variation of the apparent equilibration rate constant,  $k'$ , as a function of the  $\beta$ -Ala-CAM concentration; The reaction was performed in the presence of 400  $\mu\text{M}$  puromycin and  $\beta$ -Ala-CAM at the concentrations indicated. The  $k'$  values were estimated from the intersection point of the two linear parts of the corresponding progress curves shown in panel A.

observed (Fig. (4A)). However, these plots are distinct from those obtained with  $\beta$ -Ala-CAM; the initial slope of the progress curves does not vary as a function of the inhibitor concentration. Only the second phase follows competitive kinetics (Fig. (4B)). This finding combined with the fact that the plot of  $k'$  versus the inhibitor concentration is linear (Fig. (4C)), suggests that Phe-Phe-CAM binds to complex C in a single-step process, following the kinetic Scheme 2.

Therefore, the data can be fitted to:

$$k' = k_{off} + k'_{on}[I] \quad (3)$$

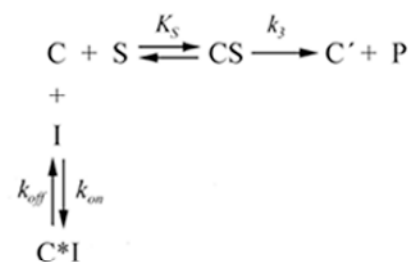
where  $k_{off}$  and  $k'_{on}$  are the dissociation and association rate constants, respectively. The  $k_{off}$  value is determined from the interception of the y-axis in Fig. (4C), while the  $k'_{on}$  is estimated from the slope of the plot and then corrected for substrate competition, using:

$$k'_{on} = k_{on}(1 + [S]/K_s) \quad (4)$$

The ratio  $k_{off}/k_{on}$  gives a value of  $K_i^*$  equal to 45,46  $\mu$ M, which is in agreement with the value 46  $\mu$ M calculated directly from the double-reciprocal plot shown in Fig. (4B). Values of the kinetic constants for inhibition of the puromycin reaction by Phe-Phe-CAM are given in Table 1.

## DISCUSSION

Localization of CAM binding sites on the ribosome is a prerequisite for formulating a hypothesis explaining the competitive type of inhibition caused by the drug on peptide-bond formation and interpreting the footprinting pattern of CAM. Although X-ray crystallographic data of CAM complexed to 50S subunits or 70S ribosomes from bacteria [12-



**Scheme 2.** Kinetic model for the inhibition of the puromycin reaction by Phe-Phe-CAM. Symbols: C, poly(U)-programmed ribosomes from *E. coli*, bearing AcPhe-tRNA at the P-site; S, puromycin; P, AcPhe-puromycin; C', a form of complex C not recycling; I, Phe-Phe-CAM

14] and chemical footprints produced by CAM at A2451, G2505 and U2506 [17, 18] under conventional experimental conditions are compatible with CAM binding at the catalytic center of the large ribosomal subunit, they are difficult to reconcile with the altered reactivities against DMS of A2058 and A2059, both placed at the entrance of the peptide exit tunnel. Such footprinting heterogeneity could correlate with more than one molecule of CAM participating or by allosteric effects transmitted from the binding site of CAM to the entrance of the exit tunnel. Although the former hypothesis is supported by previous binding studies, suggesting two CAM binding sites on the ribosome [21], it fails to explain the kinetic data of the present study. According to our kinetic model, binding of CAM at the initial (CI complex) and the final position (C\*I complex) is mutually exclusive, which means that only one molecule of CAM participates in the

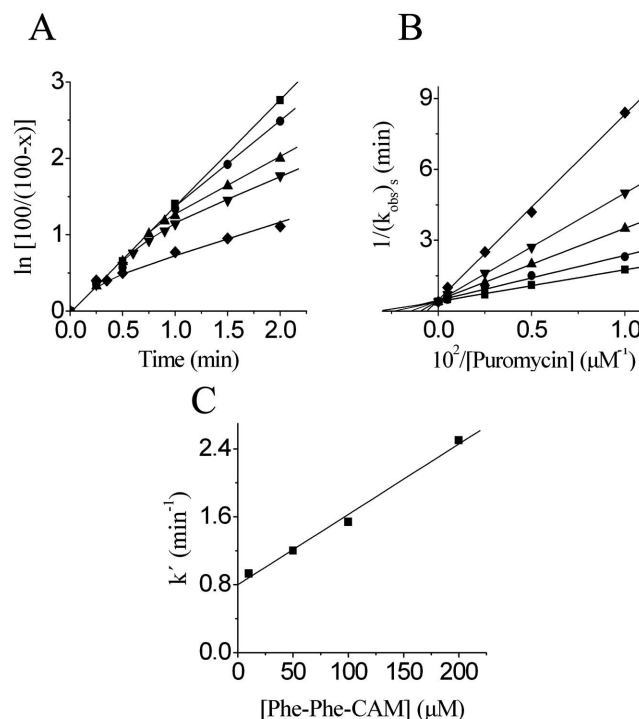


**Fig. (4).** Kinetics for the AcPhe-puromycin synthesis in the presence or absence of Phe-Phe-CAM. **A**, First-order time plots; Complex C reacted at 25 °C with (■) 400  $\mu$ M puromycin or with a solution containing 400  $\mu$ M puromycin and Phe-Phe-CAM at (●) 10  $\mu$ M, (▲) 50  $\mu$ M, (▼) 100  $\mu$ M and (◆) 200  $\mu$ M. **B**, Double-reciprocal plots; The data were collected from the late phase of logarithmic time plots, such as those shown in panel A. **C**, Variation of the apparent equilibration rate constant,  $k'$ , as a function of the Phe-Phe-CAM concentration; The reaction was performed in the presence of 400  $\mu$ M puromycin and Phe-Phe-CAM at the concentrations indicated.

mechanism of inhibition of the peptide bond formation. The reason we fail to identify kinetically the binding site of CAM at the entrance of the peptide exit tunnel, may be the low affinity of this site. As estimated by Long and Porse [20], the value of  $K_D$  equals 300  $\mu\text{M}$  and correlates with CAM binding to the weaker of the two sites ( $K_D = 200 \mu\text{M}$ ), characterized in *E. coli* by equilibrium dialysis measurements [21]. On the other hand, considering the size of CAM, it is difficult to understand how a molecule of the drug bound at the entrance of the exit tunnel can perturb the aminoacyl termini of bound tRNAs, unless allosteric conformational changes are triggered.

In the present study, we used a fast chemical-modification methodology to provide time-resolved footprinting of CAM binding to an initiator ribosomal complex derived from *E. coli*. In the encounter complex CI, CAM binding strongly protects nucleotides clustered around the hydrophobic crevice of the A-site in the large ribosomal subunit. These footprints represent a minimal estimate of the number of drug-induced effects because of technical limitations. For instance, protection at C2452 is difficult to be detected, due to the weak reactivity of cytidine with DMS [30]. Moreover, post-transcriptionally modified bases, like  $m^6\text{A}2503$  may mask drug-induced effects [31]. However, both nucleotides C2452 and A2503 are implicated in CAM binding, as deduced by crystallography [12-14] and mutagenesis [31] studies. The footprinting pattern of complex CI differs from those previously reported [17, 18], given that drug-induced effects at A2058, A2059 and A2062 are absent. Nevertheless, this footprinting pattern suggests that CAM binds adjacently to the crevice of A-site on the 50S ribosomal subunit. Accommodation of CAM at its final position (complex C<sup>\*</sup>I) favors drug's interaction with A2062. Meanwhile, the protection at G2505 and U2506 softens, a new footprint at A2059 is raised, and the reactivity of A2058 is enhanced. The footprinting pattern of complex C<sup>\*</sup>I resembles better than the CI pattern to that published by others [17, 18] and generally correlates well with recent crystallographic data [13, 14]. This may be due to the fact that both footprinting and crystallographic analyses have been performed by incubating ribosomes with CAM for prolonged time. We can rationalize our findings by suggesting a two-step mechanism of binding, where initially CAM binds deep in the A-site crevice, with its nitrobenzene ring entering the cleft formed between U2506 and G2505. Then, the molecule of CAM slowly seeks out its final position to contact the exocyclic amine of A2062. The latter nucleotide lies midway between two hydrophobic crevices; one at the PTase center and the other at the entrance of the peptide exit tunnel (Fig. (5)). Accumulated evidence suggests that the conformation of A2062 varies, depending on whether substrates or antibiotics are bound to the ribosome [32, 33]. Consequently, it could be hypothesized that changes in reactivity of A2058 and A2059 against DMS may not be due to direct effects of CAM binding but instead may be due to allosteric effects transmitted through a signal exchange network shown in Fig. (5) by successive arrows, in which A2062 processes a pivotal role. The same hypothesis may be also used to explain why CAM enhances the release of oligo(Phe)-tRNAs from the P-site [7].

Substitution of the dichloroacetyl tail of CAM, by  $\beta$ -alanyl or phenylalanyl-phenylalanyl group renders the drug less effective in inhibiting the puromycin reaction. Substitution by  $\beta$ -alanyl causes a 57-fold increase in  $K_i$  value, without affecting seriously the subsequent slow isomerization step (Table 1). This finding suggests that such substitution may lower CAM affinity by preventing the drug from fitting into its initial binding position. Similar effects on  $K_i$  value by replacement of the dichloroacetyl group of CAM with other aminoacyl groups have been observed previously [23, 34]. The present results combined with these earlier observations verify the hypothesis that the critical parameter that influences the initial binding of CAM is not the electronic structure of the aminoacyl group but rather the stereospecificity of this moiety. Substitution by a bulkier group, such as Phe-Phe, does not allow CAM binding to its initial position for steric reasons, while slows down its accommodation to the final position, probably by preventing the Phe-Phe group from hydrogen bonding with the exocyclic amine of A2062.

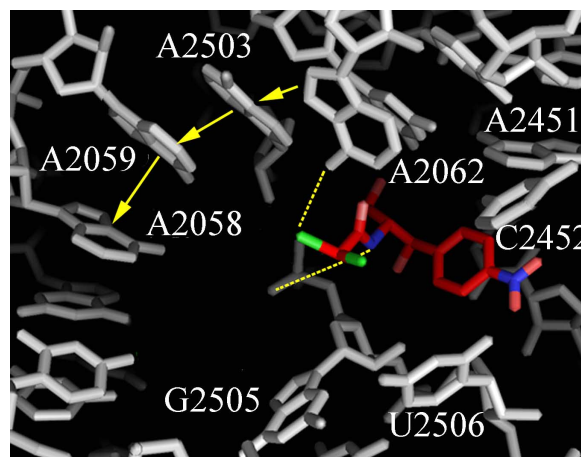


**Fig. (5).** Binding position of CAM on the *E. coli* ribosome, as detected by crystallography, PDB ID code 30FC [14]. Hydrogen bonds are shown as yellow dashes, while allosteric effects transmitted through a putative signal exchange network are indicated by successive arrows. Figure was made using Visual Molecular Dynamics (VMD).

## CONCLUSIONS

CAM behaves as a slow binding inhibitor, following a two-step mechanism. Time-resolved binding of CAM to *E. coli* ribosomes demonstrates that the principal binding site of the antibiotic is placed at the A-site of the large ribosomal subunit. Footprints of the drug at the entrance of the peptide exit tunnel do not relate to direct interactions of CAM with its region, but to allosteric effects transmitted *via* the flexible nucleotide A2062. Substitution of the dichloroacetyl tail of CAM by an aminoacyl and a dipeptidyl group not only decreases its affinity for the ribosome, but also alters the mechanism of binding. Along with recent crystallographic observations, this study provides a new basis to define the essential functional groups of CAM. With the purpose of improving CAM properties, monitoring both steps of drug binding to ribosomes may be a critical point for rationale design of drug derivatives. Further efforts in designing and

synthesizing new CAM derivatives with better affinity for the ribosome are in progress.

### ACKNOWLEDGEMENTS

This work was supported by the Research Committee of the University of Patras. We thank Dr Dimitrios Vahliotis for NMR analysis of the CAM derivatives, Dr George Papadopoulos for creating Fig. (5), and Dr Constantinos Stathopoulos for critical reading of the manuscript.

### ABBREVIATIONS

$\beta$ -Ala-CAM =  $\beta$ -alanyl-chloramphenicol  
CAM = chloramphenicol

CMCT = 1-cyclohexyl-3-(2-norpholinoethyl)-carbodiimide metho-*p*-toluene sulfonate  
DIPEA = diisopropyl-ethylamine  
DMF = dimethylformamide  
DMS = dimethyl sulfate  
Phe-Phe-CAM = phenylalanyl-phenylalanyl-chloramphenicol  
AcPhe-tRNA = acetylphenylalanyl-tRNA  
PTase = peptidyl transferase  
rRNA = ribosomal RNA

### APPENDIX

In Scheme 2, complex C reacts with puromycin (S) to give an inactivated ribosomal complex C' and product (P). This reaction is inhibited by Phe-Phe-CAM (I). In deriving the corresponding equations, it is assumed that the equilibrium  $C + S \rightleftharpoons CS$  is established instantaneously, while the equilibrium  $C + I \rightleftharpoons C^*I$  is established slowly. Under these assumptions, it follows that

$$[C] = \frac{K_S}{[S]}[CS] \text{ or } \frac{d[C]}{dt} = \frac{K_S}{[S]} \frac{d[CS]}{dt} \quad A1$$

$$\frac{dP}{dt} = k_3[CS] \text{ or } \frac{d^2P}{dt^2} = k_3 \frac{d[CS]}{dt} \quad A2$$

$$-\frac{d[C^*I]}{dt} = -k_{on}[C][I] + k_{off}[C^*I] \quad A3$$

From the balance equation,  $[C_o] = [C] + [CS] + [P] + [C^*I]$ , and from equations A1, A2, A3, it implies that

$$\frac{d^2P}{dt^2} = \frac{k_{off}k_3[S][C_o - P]}{K_S(1 + \frac{[S]}{K_S})} - k[CS]k_3 \quad A4$$

where:

$$k = k_{off} + \frac{\frac{k_3[S]}{K_S} + k_{on}[I]}{1 + \frac{[S]}{K_S}} \quad A5$$

Equation A4 can be also written as

$$\frac{dk_{obs}}{dt} = \frac{k_{off}k_3[S]}{K_S(1 + \frac{[S]}{K_S})} - k'k_{obs} \quad A6$$

where  $k'$  is the apparent rate constant for attainment of the steady state, related with the inhibitor and substrate concentrations by the relationship

$$k' = k_{off} + \frac{k_{on}[I]}{1 + \frac{[S]}{K_S}} \quad A7$$

By integration, equation A6 gives

$$-\frac{1}{k'} \ln \left[ \frac{k_{off}k_3[S]}{K_S(1 + \frac{[S]}{K_S})} - k'k_{obs} \right] = t + \text{integration constant} \quad A8$$

As time,  $t$ , approaches zero, there is no  $C^*I$  formation, but the equilibrium  $C + S \rightleftharpoons CS$  is attained.

Therefore, for  $t \rightarrow 0$

$$k_{obs} = (k_{obs})_o = \frac{k_3 [S]}{K_s + [S]} \quad \text{A9}$$

and

$$\text{integration constant} = -\frac{1}{k'} \ln \left[ \frac{k_{off} k_3 [S]}{K_s (1 + \frac{[S]}{K_s})} - k' (k_{obs})_o \right] \quad \text{A10}$$

Substitution of A10 into equation A8 gives

$$-k't = \ln \left[ \frac{\frac{k_{off} k_3 [S]}{k' K_s (1 + \frac{[S]}{K_s})} - k_{obs}}{\frac{k_{off} k_3 [S]}{k' K_s (1 + \frac{[S]}{K_s})} - (k_{obs})_o} \right] \quad \text{A11}$$

Equation A11 can be also written as

$$-k't = \ln \left[ \frac{(k_{obs})_s - k_{obs}}{(k_{obs})_s - (k_{obs})_o} \right] \quad \text{A12}$$

where  $(k_{obs})_s$  represents the  $k_{obs}$  at the late phase of the puromycin reaction and is related with the concentrations of substrate and inhibitor by the relationship

$$(k_{obs})_s = \frac{k_3 [S]}{K_s (1 + \frac{[I]}{K_i^*}) [S]} \quad \text{A13}$$

where:  $K_i^* = K_i \left( \frac{k_{off}}{k_{on} + k_{off}} \right)$  A14

By integration, equation A12 gives

$$\ln \frac{[C_o]}{[C_o - P]} = \ln \frac{100}{100 - x} = (k_{obs})_s t + \frac{[(k_{obs})_o - (k_{obs})_s]}{k'} (1 - e^{k't}) \quad \text{A15}$$

The curve corresponding to equation A15 has an asymptote given by the following equation

$$\ln \frac{100}{100 - x} = (k_{obs})_s t + \frac{[(k_{obs})_o - (k_{obs})_s]}{k'}$$

Consequently, the apparent equilibration rate constant,  $k'$ , can be determined from the intersection point of the two linear parts of the corresponding progress curve.

## REFERENCES

- [1] Yuan ZR, Shi Y. Chloramphenicol induces abnormal differentiation and inhibits apoptosis in activated T cells. *Cancer Res* 2008; 68: 4875-81.
- [2] Brown L. Resistance to ocular antibiotics: an overview. *Clin Exp Optom* 2007; 90: 258-62.
- [3] Pestka S. Studies on the formation of transfer ribonucleic acid-ribosome complexes. VII. Survey of the effect of antibiotics of *N*-acetyl-phenylalanyl-puromycin formation: possible mechanism of chloramphenicol action. *Arch Biochem Biophys* 1970; 136: 80-8.
- [4] Fernandez-Muñoz R, Vazquez D. Kinetic studies of peptide bond formation. Effect of chloramphenicol. *Mol Biol Rep* 1973; 1: 75-9.
- [5] Drainas D, Kalpaxis DL, Coutsogeorgopoulos C. Inhibition of ribosomal peptidyltransferase by chloramphenicol. Kinetic studies. *Eur J Biochem* 1987; 164: 53-8.
- [6] Xaplanteri MA, Andreou A, Dinos GP, Kalpaxis DL. Effect of polyamines on the inhibition of peptidyltransferase by antibiotics: revisiting the mechanism of chloramphenicol action. *Nucleic Acids Res* 2003; 31: 5074-83.
- [7] Rheinberger HJ, Nierhaus KH. Partial release of AcPhe-Phe-tRNA from ribosomes during poly(U)-dependent poly(Phe) synthesis and the effects of chloramphenicol. *Eur J Biochem* 1990; 193: 643-50.
- [8] Kirillov S, Porse BT, Vester B, Woolley P, Garrett RA. Movement of the 3'-end of tRNA through the peptidyltransferase centre and its inhibition by antibiotics. *FEBS Lett* 1997; 406: 223-33.
- [9] Caskey CT, Beaudet AL. Antibiotic inhibitors of peptide termination. In: Munoz E, Garcias-Fernandez F, Vazquez D, Eds. *Molecular Mechanisms of Antibiotic Action on Protein Biosynthesis and Membranes*. Amsterdam: Elsevier 1971; pp. 326-36.
- [10] Polacek N, Gomez MJ, Ito K, Xiong L, Nakamura Y, Mankin A. The critical role of the universally conserved A2602 of 23S ribosomal RNA in the release of the nascent peptide during translation termination. *Mol Cell* 2003; 11: 103-12.
- [11] Fernandez-Munoz R, Monro RE, Torres-Pinedo R, Vazquez D. Substrate and antibiotic binding sites at the peptidyl-transferase centre of *Escherichia coli* ribosomes. Studies on the chloramphenicol, lincomycin and erythromycin sites. *Eur J Biochem* 1971; 23: 185-93.
- [12] Schlünzen F, Zarivach R, Harms J, *et al.* Structural basis for the interaction of antibiotics with the peptidyl transferase centre in eubacteria. *Nature* 2001; 413: 814-21.
- [13] Bulkley D, Innis CA, Blaha G, Steitz TA. Revisiting the structures of several antibiotics bound to the bacterial ribosome. *Proc Natl Acad Sci USA* 2010; 107: 17158-63.

- [14] Dunkle JA, Xiong L, Mankin AS, Cate JH. Structures of the *Escherichia coli* ribosome with antibiotics bound near the peptidyl transferase center explain spectra of drug action. *Proc Natl Acad Sci USA* 2010; 107: 17152-57.
- [15] Triman KL. Mutational analysis of 23S ribosomal RNA structure and function in *Escherichia coli*. *Adv Genet* 1999; 41: 157-95.
- [16] Persaud C, Lu Y, Vila-Sanjurjo A, Campbell JL, Finley J, O'Connor M. Mutagenesis of the modified bases, m<sup>3</sup>U1939 and  $\psi$ 2504, in *Escherichia coli* 23S rRNA. *Biochem Biophys Res Commun* 2010; 392: 223-27.
- [17] Moazed D, Noller HF. Chloramphenicol, erythromycin, carbomycin and veramycin B protect overlapping sites in the peptidyl transferase region of 23S ribosomal RNA. *Biochimie* 1987; 69: 879-84.
- [18] Rodriguez-Fonseca C, Amils R, Garrett RA. Fine structure of the peptidyl-transferase centre on 23S-like rRNAs deduced from chemical probing of antibiotic-ribosome complexes. *J Mol Biol* 1995; 247: 224-35.
- [19] Hansen JL, Ippolito JA, Ban N, Nissen P, Moore PB, Steitz TA. The structures of four macrolide antibiotics bound to the large ribosomal subunit. *Mol Cell* 2002; 10: 117-28.
- [20] Long KS, Porse BT. A conserved chloramphenicol binding site at the entrance to the ribosomal peptide exit tunnel. *Nucleic Acids Res* 2003; 31: 7208-15.
- [21] Pongs O. Chloramphenicol. In: Hahn FE, Ed. *Antibiotics*, New York: Springer-Verlag 1979; pp. 26-42.
- [22] Anderson GW, Zimmerman JE, Callahan FM. The use of esters of *N*-hydroxysuccinimide in peptide synthesis. *J Am Chem Soc* 1964; 86: 1839-42.
- [23] Drainas D, Mamos P, Coutsogeorgopoulos C. Aminoacyl analogs of chloramphenicol: examination of the kinetics of inhibition of peptide bond formation. *J Med Chem* 1993; 36: 3542-45.
- [24] Dinos G, Wilson DN, Teraoka Y, *et al.* Dissecting the ribosomal inhibition mechanisms of edeine and pactamycin: the universally conserved residues G693 and C795 regulate P-site RNA binding. *Mol Cell* 2004; 13:113-24.
- [25] Petropoulos AD, Kouvela EC, Dinos GP, Kalpaxis DL. Stepwise binding of tylosin and erythromycin to *Escherichia coli* ribosomes, characterized by kinetic and footprinting analysis. *J Biol Chem* 2008; 283: 4756-65.
- [26] Stern S, Moazed D, Noller HF. Structural analysis of RNA using chemical and enzymatic probing monitored by primer extension. *Methods Enzymol* 1988; 164: 481-89.
- [27] Morrison JF, Walsh CT. The behavior and significance of slow-binding enzyme inhibitors. *Adv Enzymol Relat Areas Mol Biol* 1988; 61: 201-301.
- [28] Petropoulos AD, Kouvela EC, Starosta AL, Wilson DN, Dinos GP, Kalpaxis DL. Time-resolved binding of azithromycin to *Escherichia coli* ribosomes. *J Mol Biol* 2009; 385: 1179-92.
- [29] Hennelly SP, Antoun A, Ehrenberg M, *et al.* A time-resolved investigation of ribosomal subunit association. *J Mol Biol* 2005; 346: 1243-58.
- [30] Egebjerg J, Larsen N, Garrett RA. Structural map of 23S rRNA. In: Hill WE, Moore PB, Dahlberg A, Schlessinger D, Garrett RA, Warner JB, Eds. *The ribosome: structure, function and evolution*. Washington: Am Soc Microbiol 1990; pp. 168-79.
- [31] Kehrenberg C, Schwarz S, Jacobsen L, Hansen LH, Vester B. A new mechanism for chloramphenicol, florfenicol and clindamycin resistance: methylation of 23S ribosomal RNA at A2503. *Mol Microbiol* 2005; 57: 1064-73.
- [32] Hansen JL, Schmeing TM, Moore PB, Steitz TA. Structural insights into peptide bond formation. *Proc Natl Acad Sci USA* 2002; 99: 11670-75.
- [33] Mankin AS. Macrolide myths. *Curr Opin Microbiol* 2008; 11: 414-21.
- [34] Michelinaki M, Mamos P, Coutsogeorgopoulos C, Kalpaxis DL. Aminoacyl and peptidyl analogs of chloramphenicol as slow-binding inhibitors of ribosomal peptidyltransferase: A new approach for evaluating their potency. *Mol Pharmacol* 1997; 51: 139-46.

---

Received: January 25, 2011

Revised: February 25, 2011

Accepted: February 28, 2011

© Kostopoulou *et al.*; Licensee *Bentham Open*.This is an open access article licensed under the terms of the Creative Commons Attribution Non-Commercial License (<http://creativecommons.org/licenses/by-nc/3.0/>) which permits unrestricted, non-commercial use, distribution and reproduction in any medium, provided the work is properly cited.